J Mater Sci (2022) 57:7491–7502

Chemical routes to materials

Eco-friendly approach for preparation of hybrid silica aerogel via freeze drying method

Shengnan Zhai[1,2], Kejing Yu[3], Chaoran Meng[1,2], Hongbo Wang[1,2,*], and Jiajia Fu[1,2,*]

[1] Jiangsu Engineering Technology Research Centre of Functional Textiles, Jiangnan University, Wuxi 214122, China
[2] Education Ministry Ley Laboratory of Science & Technology for Eco-Textiles, Jiangnan University, Wuxi 214122, China
[3] Key Laboratory of Eco-Textile of Ministry of Education, Jiangnan University, Wuxi 214122, China

Received: 10 August 2021
Accepted: 16 December 2021
Published online: 15 April 2022

ABSTRACT

In this paper, an eco-friendly method of producing hybrid silica aerogels by freeze-drying method (FD) is proposed. In the freeze-drying system, deionized water was the only solvent, hybrid aerogels were prepared by acid–base catalysis and sol–gel method using methyltrimethoxysilane (MTMS) and water–glass as co-precursors. The microstructure, specific surface area, pore size distribution and thermal properties of the hybrid aerogels were characterized and analyzed. It was found that all samples exhibited the dual-mesoporous structures, and the molar ratio of co-precursors had a significant effect on the performance of aerogels. The tap density decreased and the porosity increased with the increase in the molar ratio of MTMS, while the thermal diffusion coefficient and thermal conductivity of aerogel decreased first and then increased. Especially when the molar ratio is 2.0, the hybrid aerogels exhibited excellent insulation performance, such as thermal diffusion coefficient of 0.0183 mm s^{-1}, thermal conductivity of 0.0460 W(m k)$^{-1}$ and great thermal stability up to 540 °C. It illustrates that hybrid aerogels have broad application prospects as insulation materials.

Introduction

Silica aerogel is an excellent nanoporous material, which owns the unique properties of low density (1–500 kg m^{-3}), high porosity (80–99.8%), high specific surface area (200–1000 m^2 g^{-1}) and low thermal conductivity (0.005–0.021 W (m K)$^{-1}$) [1, 2]. It has attracted substantial attention in aerospace, industry, construction, food packaging and many other fields, etc [3–5]. However, the extensive commercial application of aerogels in these fields has been greatly limited due to its lengthy solvent exchange process and harmful organic solvents used

Handling Editor: Chris Cornelius.

Address correspondence to E-mail: wxwanghb@163.com; jiajiafu@jiangnan.edu.cn

https://doi.org/10.1007/s10853-021-06835-9

in surface modification process, costly raw materials, as well as the complex supercritical drying technique [6, 7].

To avoid the lengthy solvent exchange process and the use of toxic solvents, aerogels without additional surface modification have been extensively studied [8], especially for hybrid aerogels. Cheng et al. prepared monolithic aerogels under ambient pressure using MTMS as precursor and reducing the process from regular three days to 5 h [9]. However, the high price of organicsilane limits the application of aerogels. Therefore, Li et al. prepared hybrid silica aerogel under ambient pressure based on MTMS and TEOS co-precursors with thermal stability of 508°C and thermal conductivity of 0.027 W $(m{\cdot}K)^{-1}$, respectively [10]. Zhang et al. obtained hybrid silica aerogel under ambient pressure based on MTES and TEOS co-precursors with thermal stability of 489.5 °C and thermal conductivity of 0.0223 W $(m{\cdot}K)^{-1}$, respectively [11]. Nevertheless, it still inevitably requires a repetitive solvent exchange process to solve the problem of capillary pressure to the nanopores during ambient pressure drying [12, 13], while freeze drying is a relatively simpler method which can overcome the adverse impact of capillary pressure by directly sublimating the excess solvent without further solvent exchange or high pressure [14]. Thus, highly porous aerogel can be synthesized by freezing at low temperature and drying under vacuum condition [15].

Pan et al. obtained hybrid silica aerogel with excellent thermal stability and low thermal conductivity of 0.0226 W $(m\ k)^{-1}$ by FD based on MTMS and water–glass co-precursors [15]. Zhou et al. obtained hybrid silica aerogel composites with excellent thermal stability (560 C) and low thermal conductivity (0.0248 W $(m\ k)^{-1}$) by FD [16]. However, up to now, most of the research on the preparation of hybrid aerogels under freeze drying system are mainly focused on tert butyl alcohol or its cosolvent, while reports on deionized water as the sole solvent are rare. Therefore, in this study, in the freeze-drying system, deionized water was used as the only solvent, MTMS and water–glass as the co-precursor, hybrid silica aerogels were prepared by acid–base catalysis and sol–gel method. Furthermore, effects of the molar ratio of MTMS/Water glass on the microstructure, pore size distribution and thermal properties of aerogels were also investigated.

Experimental methodology

Preparation of silica aerogels

Sample preparation: Silica aerogels were synthesized through an acid–base catalyzed and sol–gel process followed by FD. Water glass (wt.: 34.2%, $Na_2O::SiO_2$ = 1:: 3.28, GHHC, provided by Guangzhou Huixin Chemical CO, Ltd., China), and MTMS (Aladdin) was used as co-precursors for the production of alcogels. Other agents such as hydrochloric acid (HCl) and ammonia (NH_4OH) (purchased from Sinopharm Chemical Reagent Co., Ltd, China) were used as acid–base catalysts. Deionized water made in the laboratory was used as solvents. All reagents were used at the analytical level.

The stepwise experimental process is shown in Fig. 1. The first step was the separate hydrolysis process of two precursors. The water glass was mixed with deionized water at a volume ratio of 1:4, and 0.5 mol L^{-1} hydrochloric acid was then added to adjust the pH to 2 to form sol A. Sol B was formed by mixing MTMS: deionized water: HCl in a molar ratio of 1:40:1.45 × 10^{-3}, stirring for 30 min. Then it was made by bathing in water at 45 °C for 30 min. Besides, 0.5 M HCl solution was also used in the multi-component solvents. The second step was the mixing of sol A and B. The molar ratio of MTMS/Water glass was defined as X. The values of X were defined as 0, 0.5, 1.0, 1.6, 2.0 and 2.9, respectively.

In 10 min, 1 mol L^{-1} ammonia was added to the mixed sol and the pH of the solution was adjusted to 6.30. Then the gels can be formed within 15 min at 45 °C water bath. The gel was sealed with deionized water and aged for 24 h at 45 °C. Later, the aging gels were put into the refrigerator and frozen at -83 °C for 6 h. Finally, the hybrid aerogels were obtained by vacuum drying for 48 h in the freeze dryer.

Methods of characterization

The microstructure of aerogels was observed by field emission scanning electron microscopy (SEM, SU8220, FEI). The pore size distribution of aerogels was measured by Brunauer–Emmett–Teller analysis (Tristar II 3020 M, Micromeritics Instrument Corporation, USA), including the specific surface area calculated by BET method and pore size distribution calculated by BJH method. The tap density of the hybrid aerogel was calculated by the weight to

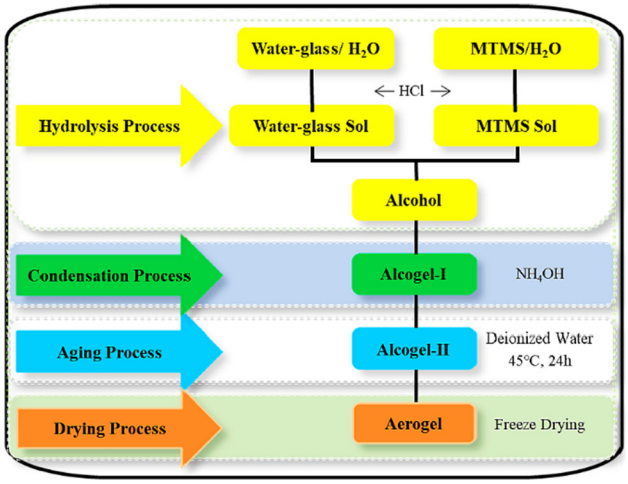

Figure 1 Experimental procedure for the synthesis of co-precursor based silica aerogels.

volume ratio, and then the porosity could be calculated by formula (A.1) [17], where ρ_s is the density of silica skeleton (2.19 g/cm^3, 25 °C, 1 atm) [18].

The chemical structure of hybrid aerogels was obtained by measuring the infrared spectra within the wavelength range of 500–4000 cm^{-1}(FTIR, Nicolet is10, Seymour Fisher Technology (China) Co., LTD). The contact angle of hybrid aerogels was measured by dropping water droplets (10 μl) on the surface of aerogel samples (DSA 100, Krüss, Germany). The thermal properties of aerogels were characterized by measuring the thermal conductivity (Hot Disk TPS 2500S, Xiaxi technology, China) and thermal diffusivity (LFA467, Nac Corporation, Germany) of materials at room temperature. The thermal stability of aerogels was characterized by measuring the weight loss of samples, heating to 800 °C at a heating rate of 10 °C/min in an oxygen atmosphere (TGA Q550).

Results and discussion

Structure analysis

Hybrid silica aerogels were formed by hydrolysis and condensation reaction of water glass and MTMS co-precursors. Reaction equations (B.1) -(B.5) explain the two different reactions with and without MTMS. Firstly, the Si $(OH)_4$ monomer molecules with silicon hydroxyl groups on the surface were formed by the hydrolysis of water glass. Then the secondary particles with large numbers of hydroxyl groups (Si–OH) on the surface were obtained by the direct condensation of these Si $(OH)_4$ molecules. However, in the presence of MTMS, the surface nonpolar group (-CH_3) was successfully added to molecules and formed relatively small secondary particles.

Figure 2a and b represent the network structures for silica aerogels with the molar ratio of 0 and 2.9, respectively. The larger secondary particles with large numbers of hydroxyl groups on the surface were connected through necks which were further growing during the aging period [19] and then mesopores were formed. The smaller secondary particles with polar groups on the surface were connected to form clusters, microspores and large pores [20].

Figure 3 represents the microstructures of hybrid aerogels with increasing molar ratio. A dense arrangement of larger particles was observed in aerogel prepared by pure water glass, which is caused by the large number of silanol groups (Si–OH) on the surface (as shown in Fig. 3a). With the increasing of mole ratio of MTMS, larger clusters and pores were observed in aerogels. When the molar ratio reached 2.0, the size and distribution of nanoparticles in the gel were more uniform (as shown in Fig. 3b–f). As a result, the color of gel with increasing molar ratio changed from transparent blue to opaque oyster white, reflecting the pore size distribution (as shown in Fig. 4).

Pore size distribution

Table 1 lists the characteristics of samples with molar ratios from 0 to 2.9, such as specific surface area, pore volume and average pore size. The minimum surface area of sample produced by pure water glass was 140.84 m^2/g, which was lower than that of the samples produced by co-precursors. This was caused by the negative effect of capillary pressure on the nanopores during the drying process, which leads to the larger shrinkage of aerogels, resulting in a decrease in specific surface area [16, 21]. The specific surface area of samples with molar ratios from 0.5 to 2.9 produced by co-precursors decreased from 756.86 to 456.87 m^2/g, while the pore volume and pore diameter first increased and then decreased with the increasing of MTMS in hybrid aerogels.

Figure 5 shows the N_2 adsorption–desorption isotherms curves of six hybrid aerogel samples, which exhibit a typical type IV, representing the presence of mesoporous materials [22]. The capillary

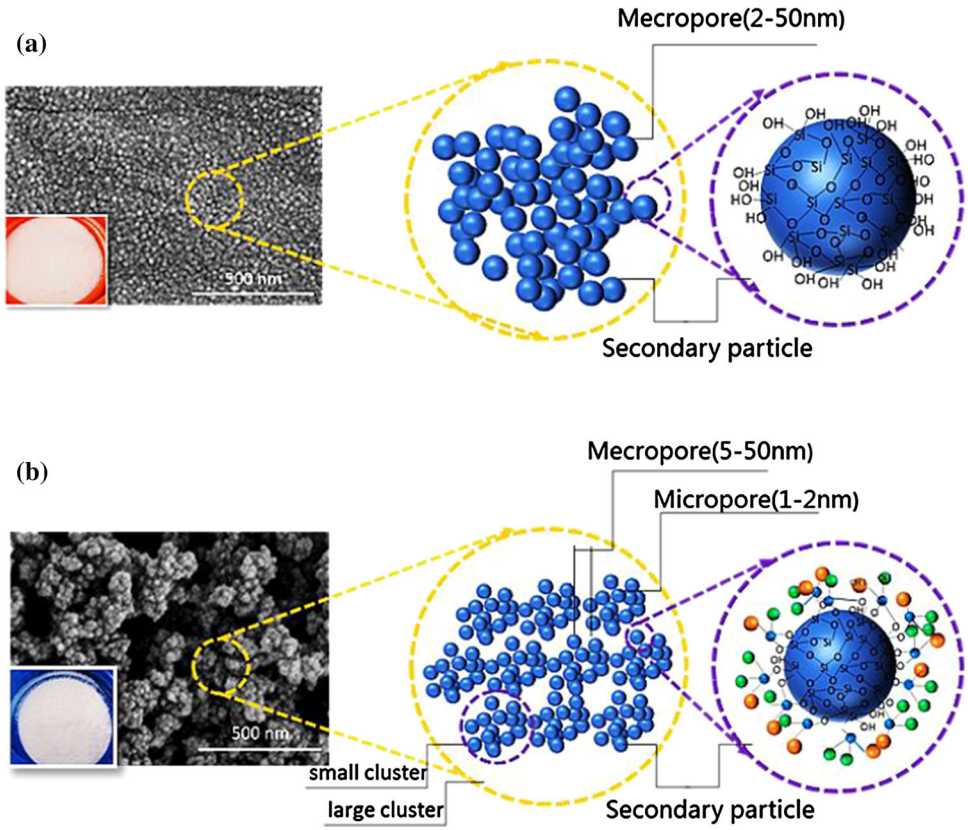

Figure 2 The formation of the gel skeleton. (a) silica aerogel prepared with pure water glass (b) silica aerogels prepared with co-precursors.

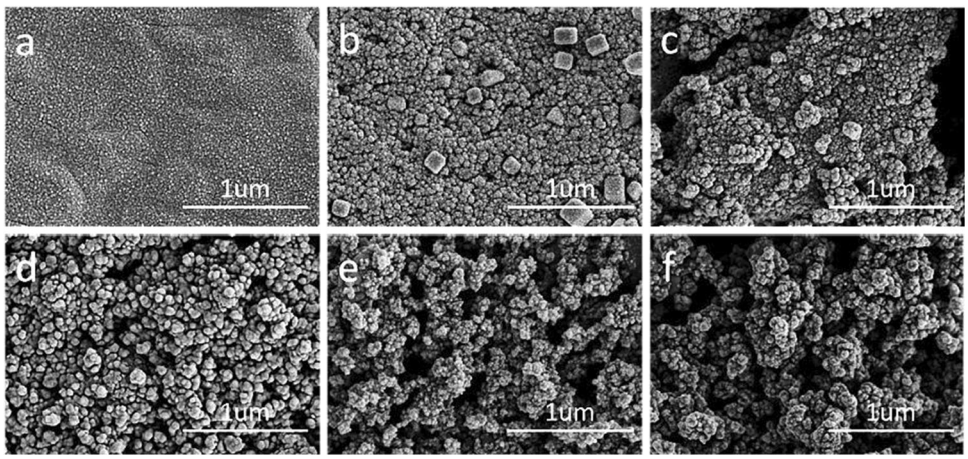

Figure 3 SEM micrographs of silica aerogels prepared with: **a** X = 0; **b** X = 0.5; **c** X = 1.0; **d** X = 1.6; **e** X = 2.0; and **f** X = 2.9.

condensation of mesopores leads to the hysteresis loops of these isotherms in the high relative pressure region. [23]. Samples with molar ratios from 0 to 1.0 exhibited identical H4 type hysteresis loops, indicating the possible presence of ink-bottle shaped pores [24], while samples with molar ratios from 1.5 to 2.9 exhibited the hysteresis loops of type H1, indicating the probable presence of cylindrical-like pores [25]. Besides, the hysteresis loops from samples with molar ratios from 2.9 to 0.5 became more obvious, which indicated that the decrease in the molar ratio leads to an increase in the number of mesopores. This could be attributed to the development and accumulation of larger secondary particles.

Figure 6 exhibits the pore size distribution of hybrid aerogels calculated by the BJH method, where macropores larger than 170 nm cannot be detected. All the samples showed the dual-mesoporous structures distributed in the range from 20 to 160 Å, including small mesoporous (25–50 Å) and large mesoporous

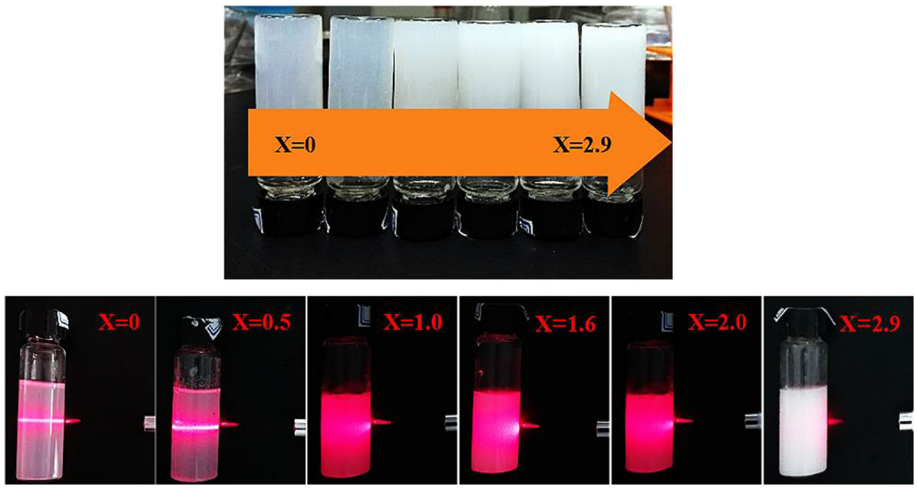

Figure 4 Gel with a series of colors prepared at different molar ratio, X = 0, 0.5, 1.0, 1.6, 2.0 and 2.9, respectively.

Table 1 A summary of properties for aerogel samples with different MTMS/Water–glass molar ratio

X	0	0.5	1.0	1.6	2.0	2.9
Specific surface area ($m^2\ g^{-1}$)	140.84 ± 5	756.86 ± 2	610.56 ± 3	564.75 ± 4	551.79 ± 2	456.87 ± 2
Pore volume ($cm^3\ g^{-1}$)	0.16 ± 1	0.74 ± 1	0.83 ± 2	0.76 ± 2	0.61 ± 2	0.46 ± 1
Average pore diameter (Å)	39.25 ± 2	42.98 ± 1	53.15 ± 3	53.66 ± 2	47.57 ± 3	45.47 ± 2

(40–160 Å). Table 2 lists the pore size distribution of samples. The sample produced by pure water glass had a minimum dV/dlog(w) pore volume value of 0.71, which was lower than that of other samples produced by co-precursors, due to pore collapse during drying process. As the molar ratio increased from 0.5 to 2.9, the pore size distribution increased and the value of dV/dlog(w) pore volume decreased from 2.50 to 1.71, indicating that the number of mesopores decreased. This was mainly attributed to the formation of macroporous structure by the accumulation of clusters in the hybrid aerogel.

Physical property analysis

Figure 7 presents the relationship between the physical properties of aerogels and different molar ratios, including gelation time, tap density, and porosity. It was obvious that gelation time increased with the increase in molar ratio, which could be attributed to the negative effect of silicon methyl on hydroxyl condensation [15]. Meanwhile, as the molar ratio of the sample increased from 0 to 2.9, the tap density decreased from 0.4340 g/cm^3 to 0.0840 g/cm^3, and the porosity increased from 80.27 to 96.18%. This was related to the capillary pressure in the drying process, and the repulsive force between methyl could effectively reduce the pore collapse [19].

FTIR analysis

Figure 8 displays the FTIR spectra which can characterize the information of chemical bond of six samples. It was known that the symmetric and asymmetric stretching vibrations of Si–O-Si bonds resulted in strong adsorption peaks at 1045 cm^{-1} and 776 cm^{-1} [26]. The deformation vibration of the adsorbed water molecules resulted in absorption peaks at 3450 cm^{-1} and 1645 cm^{-1} [27]. The stretching vibrations by Si–OH caused a weak adsorption peak at 953 cm^{-1} in the spectrum for aerogels with X increases from 0 to 1.0 [28], while the Si-CH_3 groups caused the vibration bands at 1275 cm^{-1} and 870 cm^{-1}. The peak intensity increased with the increase in the molar ratio, indicating that the number of Si-CH_3 functionalities increased with the increase in MTMS [29]. It is proportional to the contact angle of aerogel samples.

Figure 9 shows the change in contact angle of aerogels under different molar ratios, which is consistent with the analysis of IR spectra. The contact angle of aerogels increased from 0 to 51.5° with the molar ratio of MTMS/Water–glass increased from 0 to 2.9. Therefore, hydrophobic aerogels can be prepared by adjusting the molar ratio of aerogels.

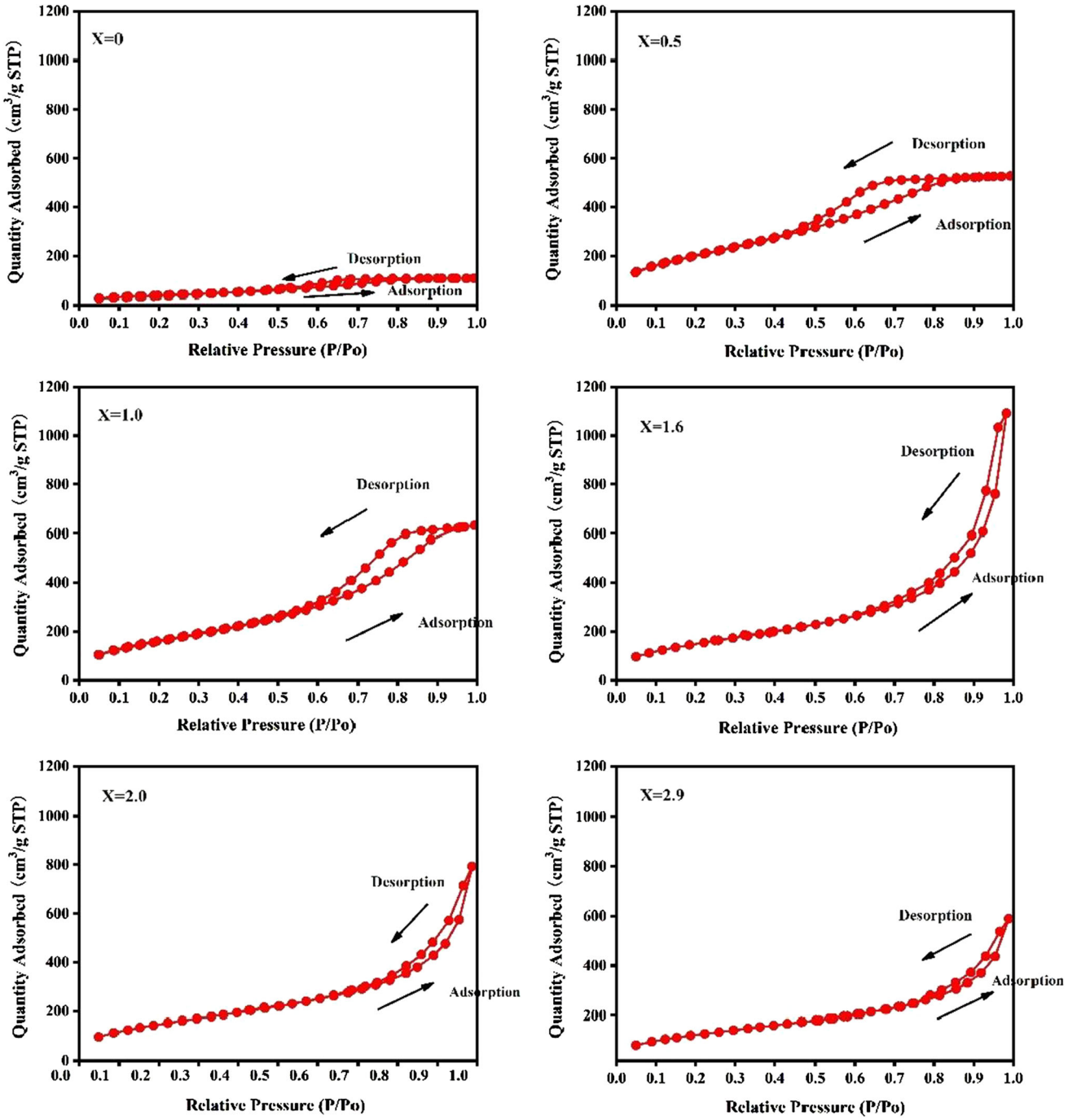

Figure 5 N_2 adsorption–desorption isotherms of co-precursor based silica aerogels prepared with various molar ratio X.

Thermal properties

Figure 10a and b shows the thermal properties of the aerogels with different molar ratios, including the thermal diffusion coefficient and the thermal conductivity. It showed that both of them first decreased and then increased when X increases from 0.5 to 2.9. At a molar ratio of 2.0, the thermal diffusion coefficient and the thermal conductivity reached the lowest values of 0.0183 $mm^2\ s^{-1}$ and 0.0460 W $(m\ k)^{-1}$, respectively. The thermal properties of aerogels decreased with the increase in MTMS content [15]. The increase in the thermal conductivity may be due to the decrease in the number of mesopores for the sample with the molar ratio of 2.9 (as shown in Table 2). Figure 10c shows the bulk density and

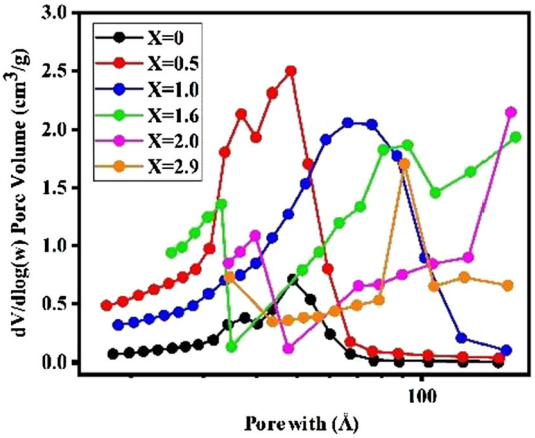

Figure 6 Pore size distribution of co-precursor based silica aerogels prepared with different X.

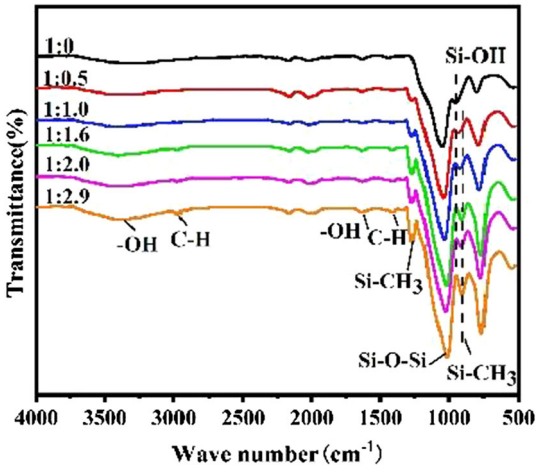

Figure 8 FTIR spectrum of six samples prepared with various molar ratio X.

thermal conductivity of different types of insulation materials [30, 31]. SiO_2 aerogels showed lower density and thermal conductivity compared with pure fiber materials. However, when introducing fiber materials into aerogels, the thermal conductivity and bulk density of composites increased significantly, especially the fiber felt aerogel composites, leading to a significant increase in transport and labor costs during practical applications. Besides, the induction of nanofibers and polymers limited the service temperature of composites, resulting in their limited application in high temperature environment.

Figure 11 shows the TG-DTG results of samples with MTMS/water glass molar ratio of 2.0 and 0, respectively. When the X value is 2.9, the curve can be

Table 2 The pore size distribution of aerogel samples with different MTMS/Water–glass molar ratio

X	small mesoporous (Å)	dV/dlog(w) Pore volume ($cm^3\ g^{-1}$)	large mesoporous (Å)	dV/dlog(w) Pore volume ($cm^3\ g^{-1}$)
0	32–40	0.29	40–65	0.71
0.5	32–45	2.20	45–65	2.50
1.0	32–37	0.70	37–125	2.06
1.5	25–35	1.29	35–160	1.90
2.0	35–48	1.09	48–160	2.25
2.9	35–40	0.73	80–110	1.71

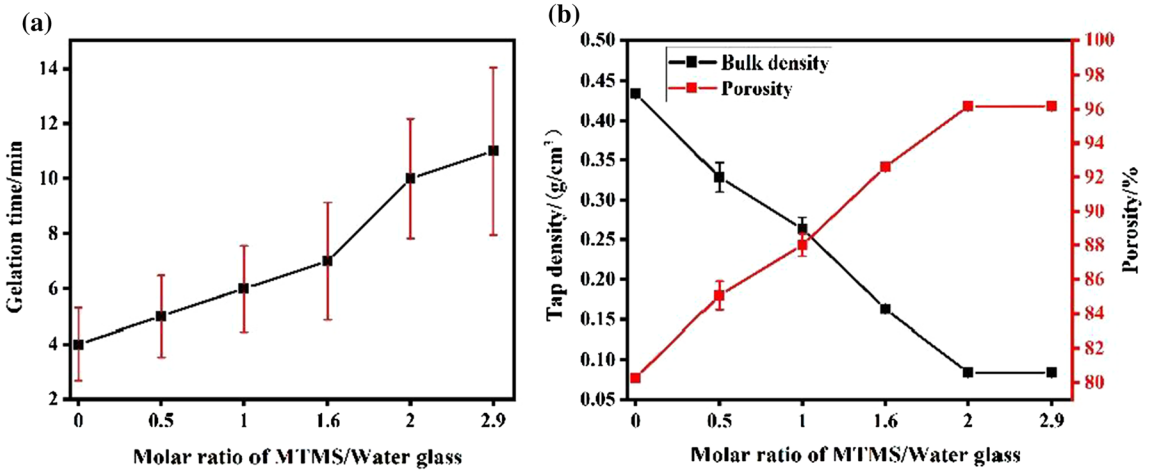

Figure 7 The effect of MTMS/Water–glass molar ratio on (**a**) gelation time; **b** tap density and porosity.

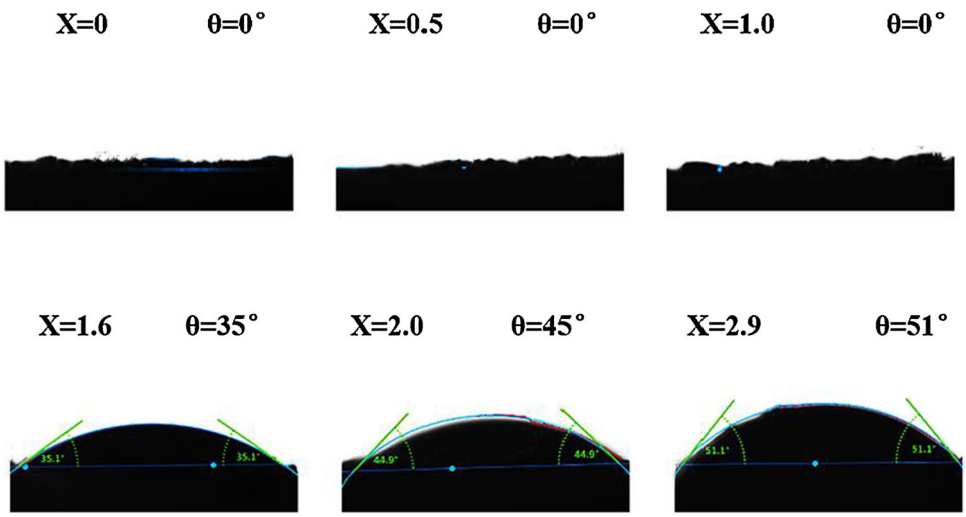

Figure 9 Contact angle of aerogel samples prepared with various molar ratio X.

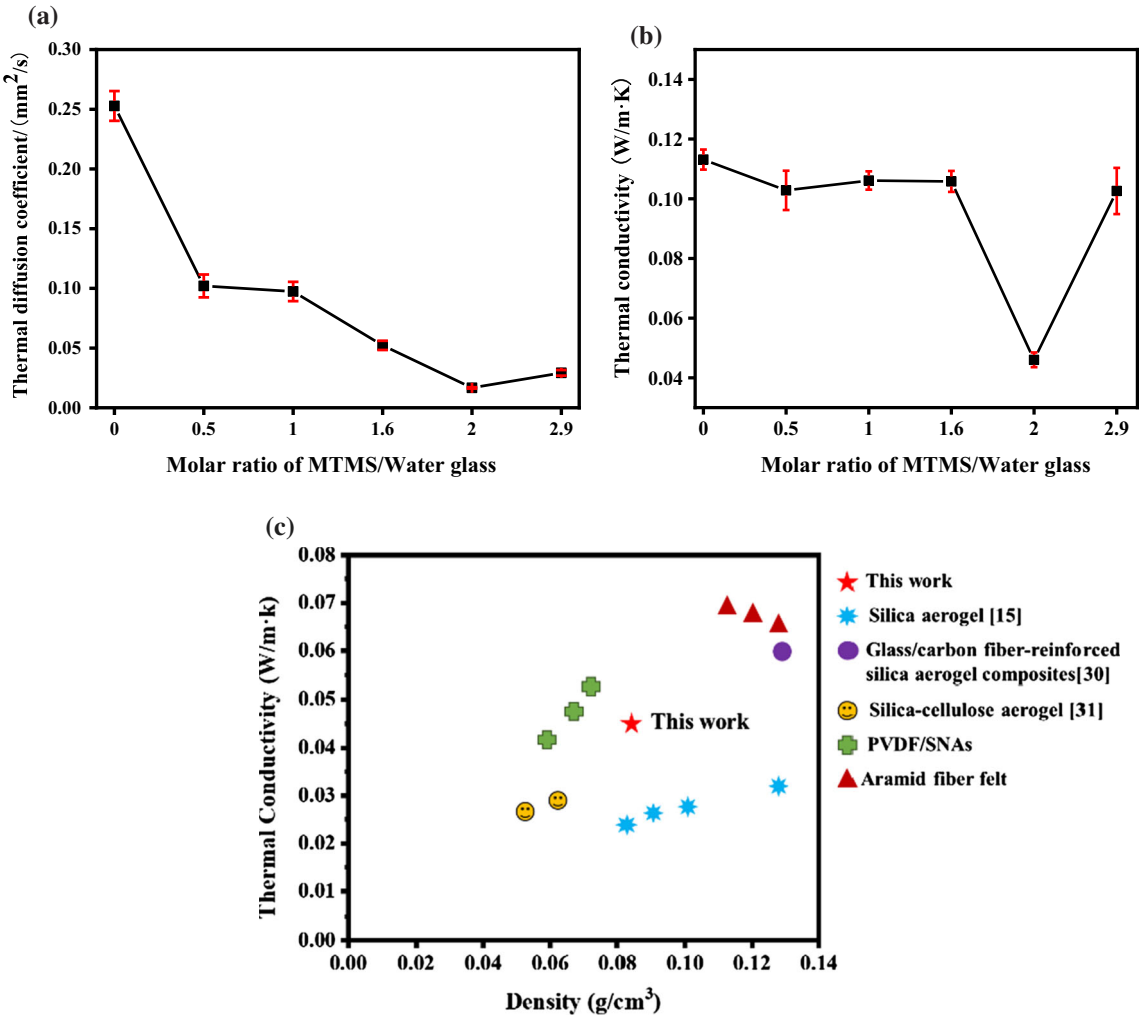

Figure 10 Thermal properties of the aerogels with different molar ratios **a** thermal diffusion coefficient and **b** thermal conductivity; **c** the relationship between density and thermal conductivity of different thermal insulation materials.

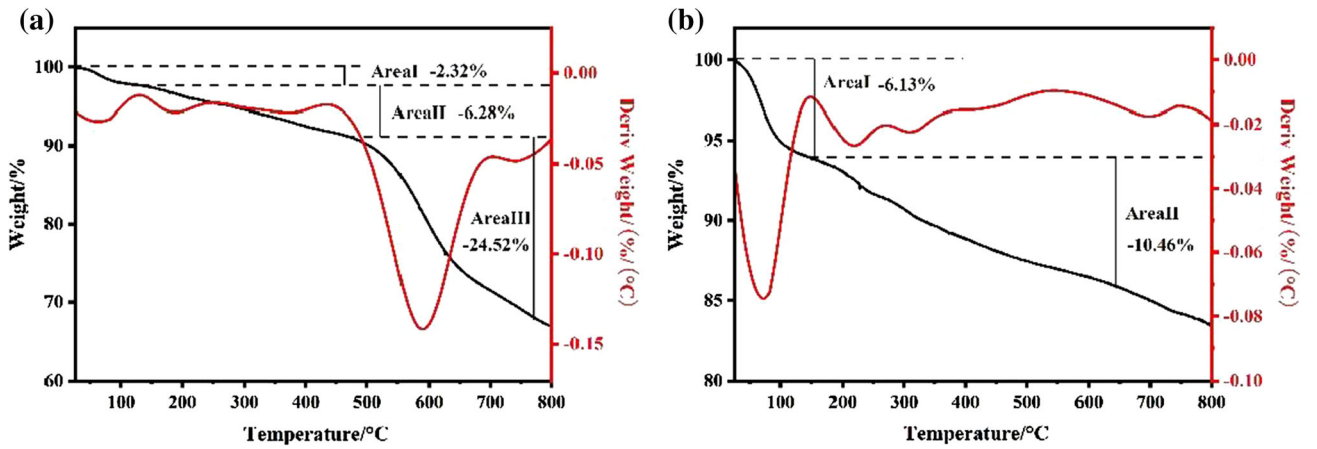

Figure 11 TG-DTG curves of co-precursor based silica aerogels prepared with: **a** X = 2.0; **b** X = 0.

divided into three stages: Area I, II and III, respectively. The first weight loss was 2.32%, which could be attributed to the evaporation of residual solvents and water molecules. The second weight loss was 6.28%, which was caused by the condensation between Si–OH [32], while the larger weight loss occurred in the third stage was due to the oxidation of Si-CH_3 [9]. Therefore, the thermal decomposition of -CH_3 begins at about 540 °C. However, there are only the first two stages of weightlessness for the samples prepared from pure water glass, due to the absence of -CH_3 groups in the aerogels. In addition, the water adsorption caused by the presence of a large amount of hydroxyl group (-OH) on the aerogel surface increased the first weight loss to 6.13%.

Conclusions

An environmentally friendly method for preparing hybrid aerogels under freeze-drying system is proposed. In the freeze-drying system, hybrid silica aerogels based on MTMS/Water glass co-precursors were prepared by acid base catalysis and gel sol method using deionized water as the sole solvent. The microstructure, pore size distribution and thermal properties of aerogels with different MTMS/Water glass molar ratios from 0 to 2.9 were systematically characterized and analyzed. The experimental results show that all samples exhibit the dual-mesoporous structures, and the molar ratio of MTMS/water glass has a great influence on the performance of the hybrid aerogels. The gelation time and porosity increased with the increase in mole ratio, while density showed the opposite trend. When the molar ratio is 2.0, the obtained hybrid aerogels boast outstanding insulation performance with low thermal diffusion coefficient (0.0183 mm s^{-1}), low thermal conductivity (0.0460 W (m k)$^{-1}$) and great thermal stability (540 °C). This method completely avoids lengthy solvent exchange, further surface modification and the use of organic solvents. It is friendly to the environment and human body.

Acknowledgements

This study was supported by the Nation Key R&D Program of China (2017YFB0309100), China Postdoctoral Science Foundation (No.2019T120390); Jiangsu Planned Projects for Postdoctoral research funds (No. 2018K018A) ; the National Natural Science Foundation of China [No.31470509] and the Key Laboratory of Eco-textiles, Ministry of Education—(supported by "the Fundamental Research Funds for the Central Universities NO. JUSRP52007A).

Declarations

Conflict of interest The authors declare that they have no conflict of interest.

Appendix 1

$$\text{Porosity} = (1 - \rho/\rho s) \times 100\% \quad (1)$$

Appendix 2

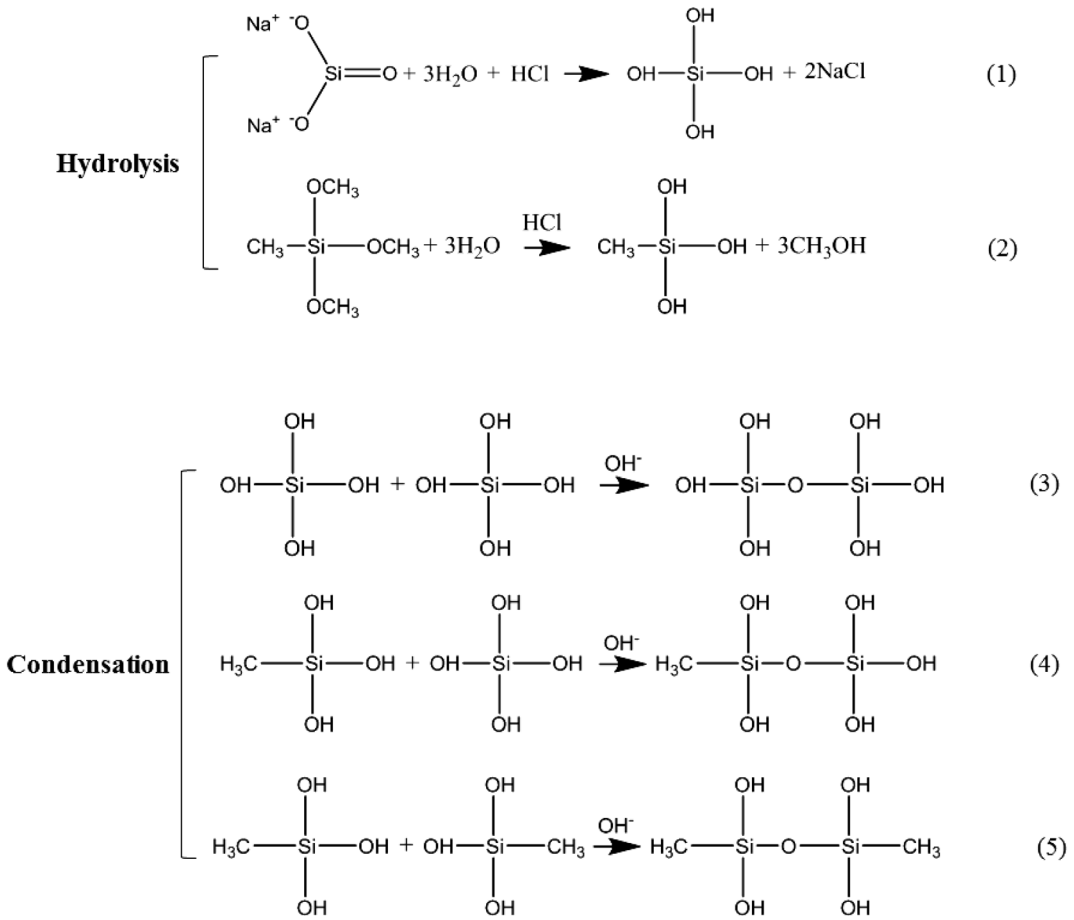

References

[1] Thapliyal PC, Singh K (2014) Aerogels as promising thermal insulating materials: an overview. J Mater 2014:127049. https://doi.org/10.1155/2014/127049

[2] Kim H, Kim K, Kim H et al (2020) Eco-friendly synthesis of water-glass-based silica aerogels via catechol-based modifier. Nanomaterials 10(12):2406. https://doi.org/10.3390/nano10122406

[3] Fricke JG (1992) Ultrasonic velocity measurements in silica, carbon and organic aerogels. J Non-Cryst Solids. https://doi.org/10.1016/S0022-3093(05)80459-4

[4] Adebajo MO, Frost RL, Kloprogge JT et al (2003) Porous materials for oil spill cleanup: a review of synthesis and absorbing properties. J Porous Mater 10(3):159–170. https://doi.org/10.1023/A:1027484117065

[5] Buratti C, Merli F, Moretti E (2017) Aerogel-based materials for building applications: influence of granule size on thermal and acoustic performance. Energy Build 152:472–482. https://doi.org/10.1016/j.enbuild.2017.07.071

[6] Shimizu T, Kanamori K, Nakanishi K (2017) Silicone-based organic-inorganic hybrid aerogels and xerogels. Chem-A European J 23(22):5176. https://doi.org/10.1002/chem.201603680

[7] Sanli D, Erkey C (2013) Monolithic composites of silica aerogels by reactive supercritical deposition of hydroxy-terminated poly(dimethylsiloxane). ACS Appl Mater Interfaces 5:11708–11717. https://doi.org/10.1021/am403200d

[8] Li M, Jiang H, Xu D et al (2016) Low density and hydrophobic silica aerogels dried under ambient pressure using a new co-precursor method. J Non-Cryst Solids 452:187–193. https://doi.org/10.1016/j.jnoncrysol.2016.09.001

[9] Cheng X, Li C, Shi X et al (2017) Rapid synthesis of ambient pressure dried monolithic silica aerogels using water

as the only solvent. Mater Lett 204:157–160. https://doi.org/10.1016/j.matlet.2017.05.107

[10] Li Z, Cheng X, He S et al (2016) Tailoring thermal properties of ambient pressure dried MTMS/TEOS co-precursor aerogels. Mater Lett 171(may15):91–94. https://doi.org/10.1016/j.matlet.2016.02.025

[11] Zhang Y, Xiang L, Shen Q et al (2020) Rapid synthesis of dual-mesoporous silica aerogel with excellent adsorption capacity and ultra-low thermal conductivity. J Non-Cryst Solids. https://doi.org/10.1016/j.jnoncrysol.2020.120547

[12] Wang J, Zhang Y, Wei Y, Zhang X (2015) Fast and one-pot synthesis of silica aerogels via a quasi-solvent-exchange-free ambient pressure drying process. Microporous Mesoporous Mater 218:192–198. https://doi.org/10.1016/j.micromeso.2015.07.019

[13] Ok SS, Gizli N (2020) Hydrophobic silica aerogels synthesized in ambient conditions by preserving the pore structure via two-step silylation-ScienceDirect. Ceram Int 46(17):27789–27799. https://doi.org/10.1016/j.ceramint.2020.07.278

[14] Freytag A, Sanchez-Paradinas S, Naskar S, N. et al (2016) Versatile aerogel fabrication by freezing and subsequent freeze-drying of colloidal nanoparticle solutions. Angew Chem Int Ed 55(3):1200–1203. https://doi.org/10.1002/anie.201508972

[15] Pan Y, He S, Gong L et al (2017) Low thermal-conductivity and high thermal stable silica aerogel based on MTMS/Water-glass co-precursor prepared by freeze drying. Mater Design 113:246–253. https://doi.org/10.1016/j.matdes.2016.09.083

[16] Zhou T, Cheng X, Pan Y et al (2017) Mechanical performance and thermal stability of glass fiber reinforced silica aerogel composites based on co-precursor method by freeze drying. Appl Surf Sci 437:321–328. https://doi.org/10.1016/j.apsusc.2017.12.146

[17] He F, Zhao H, Qu X et al (2009) Modified aging process for silica aerogel. J Mater Process Technol 209(3):1621–1626. https://doi.org/10.1016/j.jmatprotec.2008.04.009

[18] Jiang Y, Feng J, Feng J (2017) Synthesis and characterization of ambient-dried microglass fibers/silica aerogel nanocomposites with low thermal conductivity. J Sol-Gel Sci Technol 83(1):64–71. https://doi.org/10.1007/s10971-017-4383-2

[19] Dorcheh AS, Abbasi MH (2008) Silica aerogel; synthesis, properties and characterization. J Mater Process Technol 199(1–3):10–26. https://doi.org/10.1016/j.jmatprotec.2007.10.060

[20] Gurav JL, Rao AV, Nadargi DY, Park HH (2010) Ambient pressure dried TEOS-based silica aerogels: good absorbents of organic liquids. J Mater Sci 45(2):503–510. https://doi.org/10.1007/s10853-009-3968-8

[21] He J, Li XL, Su D, Ji HM, Wang XJ (2016) Ultra-low thermal conductivity and high strength of aerogels/fibrous ceramic composites. J Eur Ceram Soc 36:1487–1493. https://doi.org/10.1016/j.jeurceramsoc.2015.11.021

[22] Song H, Dongmei H, Haijiang B, Zhi L, Hui Y, Xudong C (2015) Synthesis and characterization of silica aerogels dried under ambient pressure bed on water glass. J Non-Cryst Solids 410:58–64. https://doi.org/10.1016/j.jnoncrysol.2014.12.011

[23] Sing KSW, Williams RT (2004) Physisorption hysteresis loops and the characterization of nanoporous materials. Adsorpt Sci Technol 22(10):773–782. https://doi.org/10.1260/0263617053499032

[24] Sarawade PB, Kim JK, Hilonga A et al (2011) Synthesis of hydrophilic and hydrophobic xerogels with superior properties using sodium silicate. Microporous Mesoporous Mater 139(1–3):138–147. https://doi.org/10.1016/j.micromeso.2010.10.030

[25] Rojas F, Kornhauser I, Felipe C, Esparza JM, Cordero S, Domínguez A, Riccardo JL (2002) Capillary condensation in heterogeneous mesoporous networks consisting of variable connectivity and pore-size correlation. Phys Chem Chem Phys 4:2346–2355. https://doi.org/10.1039/b108785a

[26] Stojanovic A, Comesaña SP, Rentsch D, Koebel MM, Malfait WJ (2019) Ambient pressure drying of silica aerogels after hydrophobization with mono-, di- and tri-functional silanes and mixtures thereof. Microporous Mesoporous Mater 284:289–295. https://doi.org/10.1016/j.micromeso.2019.04.038

[27] Mahadik SA, Pedraza F, Parale VG, Park H-H (2016) Organically modified silica aerogel with different functional silylating agents and effect on their physico-chemical properties. J Non-Cryst Solids 453:164–171. https://doi.org/10.1016/j.jnoncrysol.2016.08.035

[28] Zong S, Wei W, Jiang Z, Yan Z, Zhu J, Xie J (2015) Characterization and comparison of uniform hydrophilic/hydrophobic transparent silica aerogel beads: skeleton strength and surface modification. RSC Adv 5:55579–55587. https://doi.org/10.1039/c5ra08714g

[29] Yu H, Liang X, Wang J, Wang M, Yang S (2015) Preparation and characterization of hydrophobic silica aerogel sphere products by co-precursor method. Solid State Sci 48:155–162. https://doi.org/10.1016/j.solidstatesciences.2015.08.005

[30] Hung WC, Horng RS, Shia RE (2021) Investigation of thermal insulation performance of glass/carbon fiber-reinforced silica aerogel composites. J Sol-Gel Sci Technol 97:414–421. https://doi.org/10.1007/s10971-020-05444-3

[31] Chen YX, Sepahvand S, Gauvin F, Schollbach K, Yu Q (2021) One-pot synthesis of monolithic silica-cellulose aerogel applying a sustainable sodium silicate precursor. Constr Build Mater 293(11):123289. https://doi.org/10.1016/j.conbuildmat.2021.123289

[32] Huijuan L, Wei S, Cooper AT, Maohong F (2009) Preparation and characterization of a novel silica aerogel as adsorbent for toxic organic compounds. Colloids Surf A Physicochem Eng Asp 347(1–3):38–44. https://doi.org/10.1016/j.colsurfa.2008.11.033